Effect of wall heat transfer on screech in a turbulent premixed combustor

By A. Ghani†, M. Miguel-Brebion†, L. Selle†, F. Duchaine‡ AND T. Poinsot†

Large eddy simulation (LES) of adiabatic and thermally coupled walls are compared for a turbulent bluff-body flame which exhibits a strong unstable transverse mode called screech. The flame is stabilized behind a triangular flame holder. LES captures the high-frequency mode, but results depend on the condition used for heat transfer on the flame holder. Going from an adiabatic simulation to a thermally coupled case shifts the LES instability frequency: conjugate heat transfer (CHT) also modifies the limit-cycle amplitude: a decrease of 30 % of the maximal amplitude is found compared to the adiabatic LES. An active control methodology is applied to control the mode and trigger it in order to study growth rates. In the linear regime, CHT results have growth rates which are half of those obtained for the adiabatic LES. This study shows the effect of wall temperature on flame dynamics and the importance of wall temperatures for LES of combustion instabilities.

1. Introduction

Combustion releases hot gases that impact the flame holder, combustion chamber walls and turbine stages. The determination of thermal loads on these parts is crucial since they determine the design of the combustion system (Lefebvre 2010). In turn, the temperature of the flame holder has an impact on the flame, especially for turbulent applications where both high velocities and confinement ratios are encountered.

Recent numerical studies have shown the impact of thermal boundaries on laminar flames: Kaess *et al.* (2008) reported different flame-anchoring positions for adiabatic and isothermal walls with a static reference temperature. For the adiabatic case the flame root stabilized on the anchoring plate, whereas for the isothermal case the flame was lifted due to local quenching in the near-wall region. Flame root displacements control the stability of a system as demonstrated by Duchaine *et al.* (2011) who used direct numerical simulations (DNS) of acoustically perturbed flames and showed that the wall temperatures of the duct as well as the combustor were affecting the flame response. Kedia *et al.* (2011) studied a metal and a ceramic bluff-body subjected to harmonic velocity forcing. They observed significantly different dynamics of the wake flow due to conductivity changes. Similar observations were made for turbulent swirling flames (Schmitt *et al.* 2007; Tay-Wo-Chong & Polifke 2013). These studies applied isothermal boundaries where the wall temperature was evaluated approximately. The next step towards reliable simulations is the coupling of unsteady heat transfer from the reacting flow to the solid (and vice versa) in order to correctly predict the temperature in the solid.

The unsteady heat transfer between solid and gas can have several effects which are still poorly understood. Its impact on combustion instabilities is of major concern since small

† Institut de Mécanique des Fluides de Toulouse (IMFT), France
‡ CERFACS, France

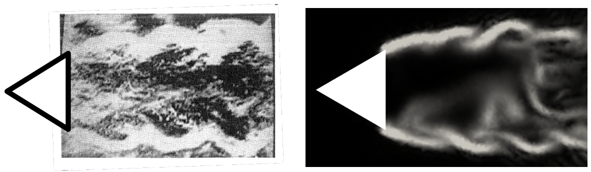

Experimental schlieren Numerical schlieren

FIGURE 1. High-frequency transverse modes in the Volvo test rig. Top: Schlieren image behind the bluff-body showing the symmetric vortex shedding due to transverse combustion instability (Sjunnesson *et al.* (1992)). Bottom: Numerical Schlieren from LES.

	Bluff-body	Chamber walls
Coupled case	Heat solver	Isothermal
Adiabatic case	Adiabatic	Adiabatic

TABLE 1. Overview of LES cases with thermal treatments at boundaries.

changes in flow and flame characteristics can change the stability of the system (Mejia *et al.* 2014). This study focuses on the influence of heat transfer on high-frequency transverse combustion instabilities (screech). From an industrial point of view, it is interesting to look at the pressure amplitudes during screech limit cycles since these are the most dangerous for the combustor. Furthermore, the impact of heat transfer on the growth rate of the unstable mode is interesting because most instability prediction methods rely on this linear and transitional phenomenon (Candel 2002; Sattelmayer & Polifke 2003). Several experimental studies on instability growth rates have been reported (Culick 1971; Poinsot *et al.* 1988; Searby 1992; Flandro 1995) but the impact of flame holder temperature on the growth rate was not discussed.

The target configuration is an afterburner configuration designed by Volvo where high-frequency transverse modes ($f_s = 1400\,\mathrm{Hz}$) were observed experimentally (Figure 1). The objective of the experiment was to build an academic test case to validate turbulent combustion models (Sjunnesson *et al.* 1991*b*, 1992, 1991*a*). Recent numerical studies focused on the unstable (acoustic and hydrodynamic) modes in this combustor (Fureby 2000; Giacomazzi *et al.* 2004; Jourdain & Eriksson 2012, 2010; Erickson & Soteriou 2011; Cocks *et al.* 2015). This paper focuses on the control of the observed transverse combustion instability and its growth rate. To do so, two independent solvers are coupled as proposed by Duchaine *et al.* (2009): Large Eddy Simulation (LES) is used for the reacting flow and an unsteady heat transfer solver for the flame holder. This coupling methodology is used to study the growth of transverse combustion instabilities: starting from the limit cycle, an active control method is applied to establish a stable flame. Next, when the control device is turned off, the instability grows in time and is measured in the linear regime. The computations are repeated for an adiabatic flame holder in order to understand the effect of the flame holder temperature (Table 1).

This paper is organized as follows: first, the configuration is described followed by the presentation of the numerical method for the flow and the solid solver. The last section presents analysis of the limit-cycles and the growth rate measurements of both cases.

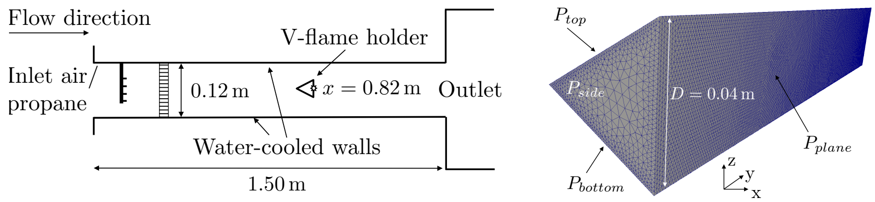

FIGURE 2. Left: Geometry of the Volvo test rig. Right: Dimension, mesh and coupled patches of the V-flame holder for solid computations. All edges of the triangle have the length D.

2. Configuration and numerical methods

The target configuration is the so-called Volvo rig installed and tested experimentally by Sjunnesson *et al.* (1991*b*, 1992, 1991*a*). The rectangular combustor has the dimensions $1.50\,\mathrm{m} \times 0.24\,\mathrm{m} \times 0.12\,\mathrm{m}$ (Figure 2 left). An equilateral triangle (edge length of $D = 0.04\,\mathrm{m}$) serves as the flame holder and is positioned at $x = 0.82\,\mathrm{m}$. The combustor can be considered as acoustically closed on both sides since air is entering through a critical plate (imposed mass flow rate) and the outlet ends in a large duct (imposed pressure).

The operating point computed with LES corresponds to the screech case (Sjunnesson *et al.* 1991*b*, 1992, 1991*a*) and was already reported numerically by Jourdain & Eriksson (2010, 2012) using URANS and Cocks *et al.* (2015); Ghani *et al.* (2015) using LES. The fuel feeding line and honeycomb are not considered in the LES since their impact on the results is marginal. A perfectly premixed propane/air mixture is injected at atmospheric pressure conditions through the inlet with $u_{bulk} = 36\,\mathrm{m/s}$, superimposed with a turbulence level of 8 % at a temperature of 288 K. Based on the edge length of the bluff body ($D = 0.04\,\mathrm{m}$), the operating point for the reacting case corresponds to a Reynolds number of ca. 5×10^4. The equivalence ratio is $\phi = 0.72$.

The reactive multi-species 3D Navier-Stokes equations are solved using a fully compressible code (Schönfeld & Rudgyard 1999; Moureau *et al.* 2005). A two-step Taylor-Galerkin finite-element convection scheme (Colin *et al.* 2000) is chosen for third-order accuracy in time and space. The subgrid stress tensor is modeled using the Sigma closure proposed by Nicoud *et al.* (2011). A two-step scheme is used for propane/air chemical kinetics: the first reaction is irreversible and controls the oxydation of fuel, while the second reaction is reversible leading to an equilibrium between CO and CO_2 (Ghani *et al.* 2015). Flame/turbulence interactions are described by the dynamic thickened flame model with the subgrid-scale efficiency model of Charlette *et al.* (2002). The Navier-Stokes Characteristic Boundary Conditions (NSCBC proposed by Poinsot & Lele (1992)) are applied to the acoustically reflecting inlet and outlet boundaries. The boundaries of the flame holder are coupled with the solid solver (coupled case), whereas the heat losses due to water-cooling at the top and bottom are modeled as no-slip isothermal walls ($T_{chamber} = 400\,\mathrm{K}$). In the adiabatic case, chamber walls as well as the flame holder are no-slip adiabatic walls (Table. 1).

The fully tetrahedral mesh contains 8 M nodes corresponding to 46 M cells. A grid width of $\Delta = 5 \times 10^{-4}\,\mathrm{m}$ in the turbulent flame brush allows reduceing the flame thickening to maximum values of $\mathcal{F} = 3$. Two additional meshes (6 M and 11 M nodes) were tested showing similar results and confirming mesh independency.

The thermal conduction code called AVTP (Duchaine *et al.* 2009) is used to compute the temperature field in the solid bluff-body by solving the unsteady energy equation and applying Fourier's law for the heat conduction term. The conjugate heat transfer problem requires coupling of the LES solver with AVTP so that each set of equations is solved by the corresponding code and communicated through the coupled patches (Figure 2, right). The extremities of the triangular flame holder are set to $T_{ends} = 350\,\mathrm{K}$, which corresponds to experimental temperature measurements. The heat flux and temperature information at the coupled patches are transferred between the two codes at fixed time steps (weakly coupled). The physical time in each code during data transfer was kept identical. The code coupling is done by using a fully parallel code coupler called PALM proposed by Piacentini *et al.* (2011). More details on the parallel conduction solver can be found in Jaure *et al.* (2013) and Duchaine *et al.* (2015).

3. Results and discussions

3.1. *Limit-cycle analysis*

First, the limit-cycle for screech during the coupled case is analyzed (Figure 3): a stable limit-cycle is established at a frequency of 1360 Hz. The phase portrait allows the phase space of the system to be analyzed: the non-linear limit-cycle forms a well-defined geometrical structure with a closed curve indicating its periodic temporal nature. Similar flow structures can be identified between the Schlieren image from experiments and the numerical Schlieren reconstructed from the divergence of the density field obtained from LES (Figure 1). Good qualitative agreement is found in terms of flame surface perturbations due to the unstable mode. The instability mechanism cycle is as follows (Figure 5, left): acoustic perturbations impinge on the flame holder and generate symmetric vortex shedding, originating from the mode conversion process at the bluff-body edge (Ghani *et al.* 2015). The vortices roll up on the flame and generate flame surface modulations which in turn act as an acoustic source, feeding the acoustic mode. Figure 5 (right) shows the correlation of flame surface and transverse velocity variations for one instability period. Variations of the flame area are known to feed the acoustic field with energy and close the feedback loop (Lieuwen 2012).

The instability mechanism remains identical for the adiabatic case (Figure 4). The amplitude of the limit cycle is ca. 30 % higher than in the coupled case. Since isothermal walls are imposed on the upper and bottom combustor walls, thermal losses will contribute to energy distribution and lead to lower pressure fluctuations (Searby *et al.* 2008; Lieuwen 2012).

The recirculation zone temperature in the coupled case (Figure 6, left) is higher than that for the adiabatic case so that a small frequency shift (10 Hz) is observed for the screech mode. The higher temperature in the burnt gases is due to the preheating effect of the fresh gases by the flame holder. The evolution of the fresh-gas temperature along the bluff-body centerline $[AB]$ (Figure 7, left) indicates a constant temperature for the adiabatic case, while an increase in temperature is exhibited for the coupled case. Nevertheless, an increasing temperature for the adiabatic case is also observed before reaching the flame foot since heat diffusion comes into play and modifies the fresh gas temperature. In the coupled case, the flame stabilizes further downstream so that the temperature increase on the flame holder is a preheating effect solely.

Figure 6 (right) displays the different flame-anchoring positions for both cases: while in the adiabatic case the flame is attached on the flame holder, the coupled case features local quenching effects and a lifted flame.

Figure 7 (middle) shows the temperature along the path $[CD]$: higher burnt gas temperatures are attained for the coupled case and finally cause the frequency shift. The

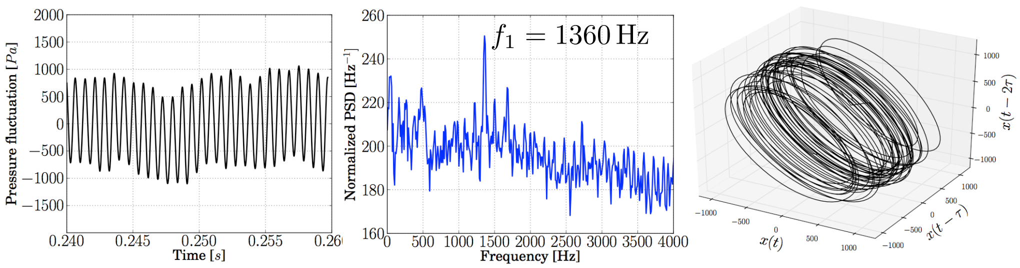

FIGURE 3. Limit cycle of the coupled case. Left: Pressure fluctuations during screech combustion. Middle: PSD of pressure signal. Right: Phase portrait of the limit cycle (Glendinning (1994)).

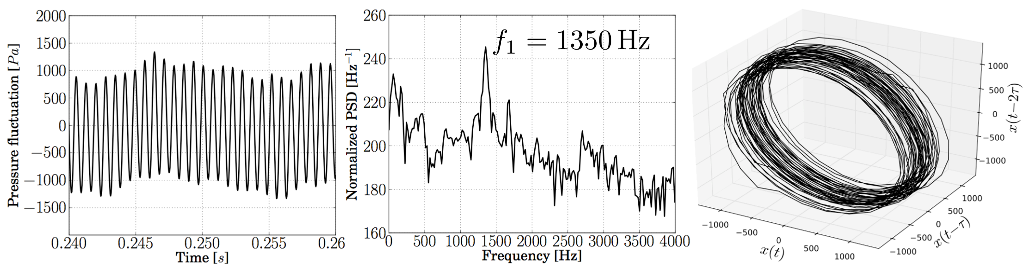

FIGURE 4. Limit cycle of the adiabatic case. Left: Pressure fluctuations during screech combustion. Middle: PSD of pressure signal. Right: Phase portrait of the limit cycle.

increased temperature of the fresh gases in the coupled case changes flame characteristics such as laminar flame velocity, flame thickness and adiabatic temperature of the burnt gases (Figure 7, right). The temperature profile of Figure 7 (middle) shows that higher temperatures are attained for the coupled case and finally cause the frequency shift.

In order to verify the link between the preheating of fresh gases to the higher burnt gas temperatures, freely propagating flames were computed using CANTERA with the GRI-MECH 3.0 mechanism. The operating conditions correspond to the LES whereby the fresh gas temperature was varied. A linear relation is found between the inlet temperature and the adiabatic flame temperature, confirming the trends observed in the LES.

3.2. *Thermal effects on the flame holder*

Figure 8 displays the temperature field in the solid for the coupled case. The temperature distribution inside the solid decreases in the upstream direction from 700 K to 400 K since it is surrounded by fresh gases. Temperatures on the top and bottom patches are on average at ca. 500 K: these patches are responsible for the preheating of the fuel-air mixture. From the fluid side, the temperatures impacting the P_{plane} for the adiabatic and coupled case are very different. While the distribution (Figure 9, left) of the adiabatic case is shifted to values corresponding to the adiabatic flame temperature, the coupled case reveals a wide temperature distribution giving an average temperature of 600 K.

Figure 9 (right) displays the integrated heat fluxes over the patches P_{side}, P_{top}, P_{bottom} and P_{plane}. The flux of the flame holder surface in the burnt gases is positive meaning that it is oriented into the solid with ca. 1350 W. This thermal power is exiting the bluff-body through the surfaces P_{top} and P_{bottom} in the zone of the fresh gases. Thermal losses

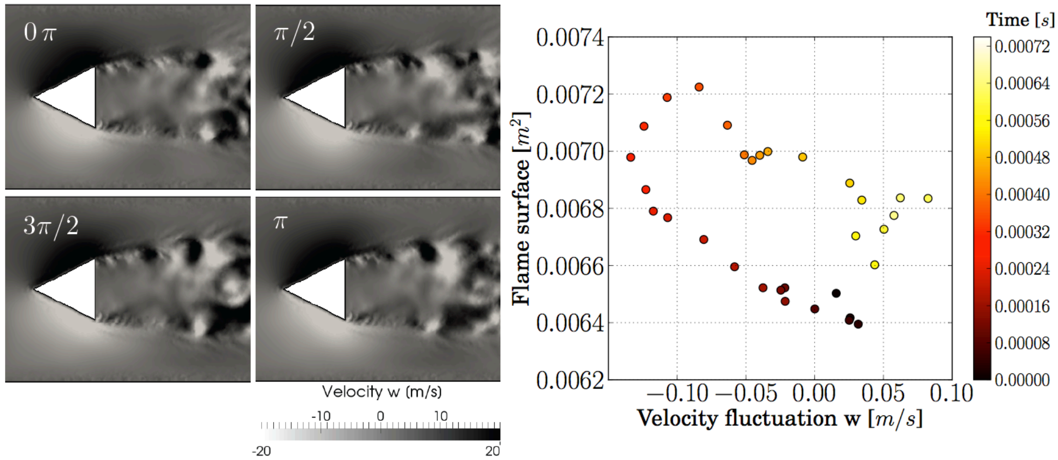

FIGURE 5. Left: Symmetric vortex pairs shed from the bluff-body edge during one screech cycle at middle-cut plane ($y = 0.12\,\mathrm{m}$). Right: Correlation between flame surface and transverse velocity fluctuations over one cycle. The iso-surface of heat release used is $5 \times 10^8\,\mathrm{W/m^3}$. The velocity fluctuations are recorded at probe position $x = 0.82\,\mathrm{m}$ and $y = 0.04\,\mathrm{m}$.

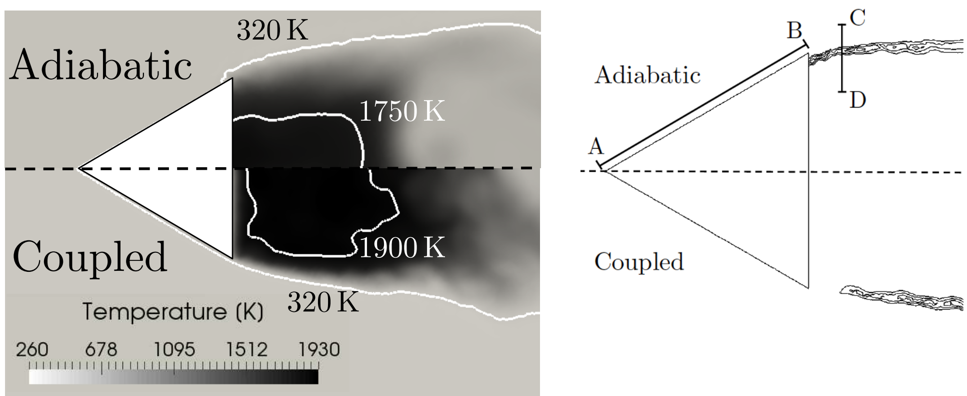

FIGURE 6. Left: Temperature fields averaged over 5 instability cycles. The adiabatic case and coupled case with the temperature profiles. Right: Instantaneous flame stabilization for the adiabatic and coupled case illustrated by heat release contours ranging from $5 \times 10^8\,\mathrm{W/m^3}$ to $1 \times 10^9\,\mathrm{W/m^3}$.

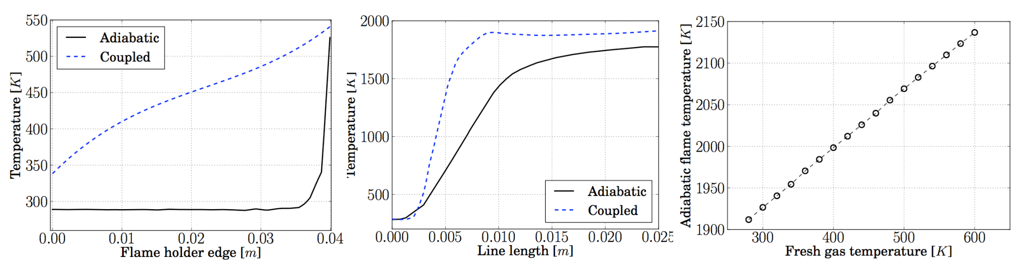

FIGURE 7. Left: Temperature profiles plotted along path $[AB]$ (Figure 6). Middle: Temperature profiles along path $[CD]$ for the adiabatic and coupled case. Right: Impact of fresh gas temperature on adiabatic flame temperature for propane using CANTERA with the GRI-MECH 3.0 mechanism at atmospheric conditions (P=1 bar).

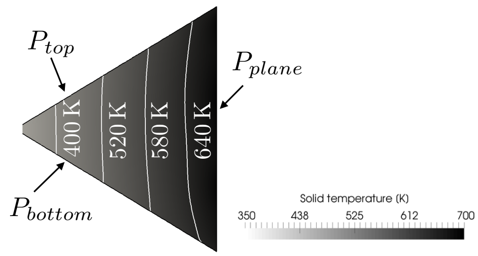

FIGURE 8. Temperature field in the solid for the coupled case.

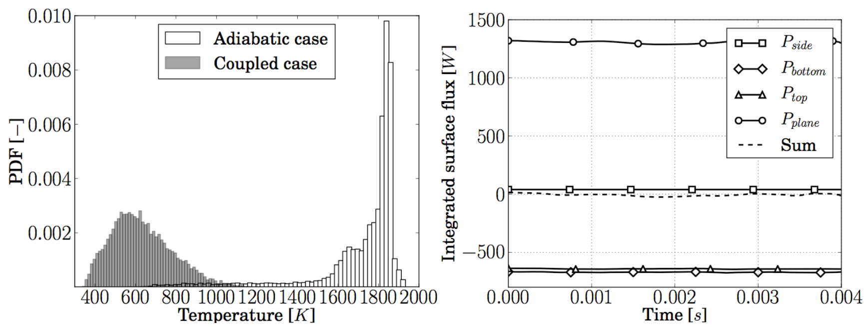

FIGURE 9. Left: PDFs of temperature of the fluid impacting the solid flame holder surface P_{plane}. Right: Integrated surface fluxes entering or exiting the bluff-body surfaces.

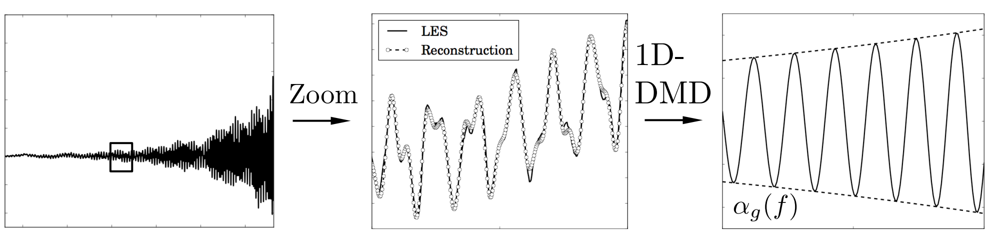

FIGURE 10. Process chart for growth rate measurement. Left: Exponential growth of the pressure signal with one time window for 1D-DMD analysis. Middle: Pressure signal encountered in LES compared to the reconstruction by the DMD including all frequencies. Right: Reconstructed signal from the 1D-DMD for the transverse mode only.

through the side boundaries are small. The balance is fluctuating around zero, indicating a converged solid solution.

3.3. *Growth rate measurement of the transverse mode*

This section focuses on the growth rates of the transverse mode at 1360 Hz. To measure these rates in the linear regime, the transverse mode has to be controlled first. An active control method for combustion instabilities has been described in Ghani *et al.* (2016): compliant walls are used on the top and bottom walls of the combustor. The wall impedance can be tuned to damp the transverse mode. This technique is used here to stabilize the instability: starting from a controlled stable regime, the active control is switched off and the transverse mode grows in time. Figure 10 describes the work process of growth rate evaluation: First, a small time frame is selected for the 1D-DMD analysis

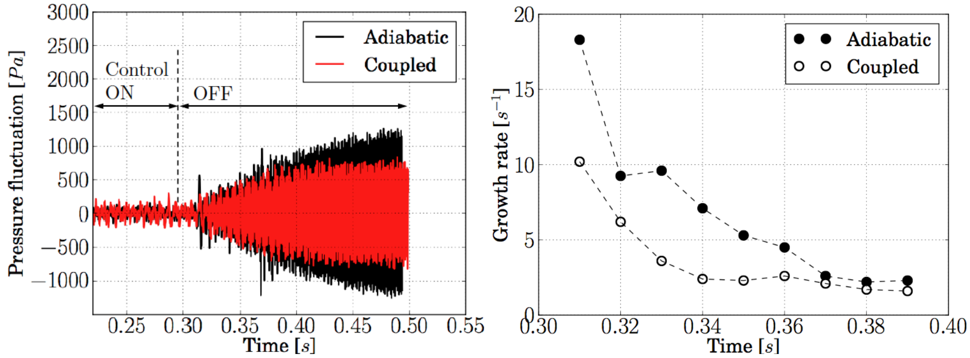

FIGURE 11. Left: Growth of the transverse mode for both cases after control of the unstable mode. Right: Measured growth rates for the adiabatic and coupled case.

(Schmid 2010). The signal is decomposed into amplitudes and phases for each frequency. It is compared to the reconstructed signal to check the quality of the DMD performance in Figure 10 (middle). In a next step, the growth rate at the frequency of the transverse mode is extracted. This procedure is done for 10 time frames in the time signal from $t = 0.30$ s to $t = 0.40$ s.

The growth rates for the adiabatic and coupled cases are different (Figure 11, left). Figure 11 (right) displays the growth rates obtained during the exponential growth of the transverse mode. The growth rate reaches its maximum shortly after the onset of the transverse pressure oscillations and decreases to zero as the mode goes towards the limit-cycle. The growth rates of the adiabatic case are higher than those of the coupled case, showing that accounting for heat transfer in the flame holder leads to a flame which is more stable than the adiabatic one.

4. Conclusions

LES of an adiabatic and thermally coupled transverse combustion instability were performed in the Volvo configuration. The comparison demonstrates significant differences in the characteristics of the unstable screech mode: while the mode frequency shifts by only 10 Hz, the growth rates and the limit-cycles are changed significantly. In the linear regime the growth rates are higher for the adiabatic case. One possible reason is the thermal dissipation in the coupled case which is not present in the adiabatic case. The limit-cycle screech amplitude is ca. 30 % lower for the coupled case. Results show that future instability studies should account for the dynamic effects of heat transfer for more realistic predictions.

REFERENCES

CANDEL, S. 2002 Combustion dynamics and control: progress and challenges. *Proc. Combust. Inst.* **29**, 1–28.

CHARLETTE, F., MENEVEAU, C. & VEYNANTE, D. 2002 A power-law flame wrinkling model for LES of premixed turbulent combustion part i: Non-dynamic formulation and initial tests. *Combust. Flame* **131**, 159–180.

Cocks, P., Soteriou, M. & Sankaran, V. 2015 Impact of numerics on the predicitive capabilities of reacting flow LES. *Combust. Flame* **162**, 3394–3411.

Colin, O., Ducros, F., Veynante, D. & Poinsot, T. 2000 A thickened flame model for large eddy simulations of turbulent premixed combustion. *Phys. Fluids* **12**, 1843–1863.

Culick, F. 1971 Non-linear growth and limiting amplitude of acoustic oscillations in combustion chambers. *Combust. Sci. Tech.* **3**, 1–16.

Duchaine, F., Boudy, F., Durox, D. & Poinsot, T. 2011 Sensitivity analysis of transfer functions of laminar flames. *Combust. Flame* **158**, 2384–2394.

Duchaine, F., Corpron, A., Pons, L., Moureau, V., Nicoud, F. & Poinsot, T. 2009 Development and assessment of a coupled strategy for conjugate heat transfer with large eddy simulation: Application to a cooled turbine blade. *Int. J. Heat Fluid Flow* **30**, 1129–1141.

Duchaine, F., Jauré, S., Poitou, D., Quémerais, E., Staffelbach, G., Morel, T. & Gicquel, L. 2015 Analysis of high performance conjugate heat transfer with the openpalm coupler. *Computational Science & Discovery* **8**, 015003.

Erickson, R. & Soteriou, M. 2011 The influence of reactant temperature on the dynamics of bluff body stabilized premixed flames. *Combust. Flame* **158**, 2441–2457.

Flandro, G. 1995 Effects of vorticity on rocket combustion stability. *J. Prop. Power* **11**, 607–625.

Fureby, C. 2000 A computational study of combustion instabilities due to vortex shedding. *Proc. Combust. Inst.* **28**, 783–791.

Ghani, A., Poinsot, T., Gicquel, L. & Müller, J.-D. 2016 LES study of transverse acoustic instabilities in a swirled kerosene/air combustion chamber. *Flow, Turb. and Combustion* **96**, 207–226.

Ghani, A., Poinsot, T., Gicquel, L. & Staffelbach, G. 2015 LES of longitudinal and transverse self-excited combustion instabilities in a bluff-body stabilized turbulent premixed flame. *Combust. Flame* **162**, 4075–4083.

Giacomazzi, E., Battaglia, V. & Bruno, C. 2004 The coupling of turbulence and chemistry in a premixed bluff-body flame as studied by LES. *Combust. Flame* **138**, 320–335.

Glendinning, P. 1994 *Stability, Instability and Chaos: An introduction to the theory of nonlinear differential equations*. Cambridge University Press.

Jaure, S., Duchaine, F., Staffelbach, G. & Gicquel, L. 2013 Massively parallel conjugate heat transfer methods relying on large eddy simulation applied to an aeronautical combustor. *Comput. Sci. & Discovery* **6**, 015008.

Jourdain, G. & Eriksson, L.-E. 2010 Combustor stability analysis based on linearized flow solvers and Arnoldi-based eigenmode extraction techniques. In *16th AIAA/CEAS Aeroacoustics Conference*, pp. 1–16.

Jourdain, G. & Eriksson, L.-E. 2012 Numerical comparison between the dynamic mode decomposition and the Arnoldi extraction technique on an afterburner test case. In *18th AIAA/CEAS Aeroacoustic Conference*, pp. 2012–2147.

Kaess, R., Polifke, W., Poinsot, T., Noiray, N., Durox, D., Schuller, T. & Candel, S. 2008 CFD-based mapping of the thermo-acoustic stability of a laminar premix burner. *Proceedings of the Summer Program*, Center for Turbulence Research, Stanford University, pp. 289–302.

Kedia, K., Altay, H. & Ghoniem, A. 2011 Impact of flame-wall interaction on premixed flame dynamics and transfer function characteristics. *Proc. Combust. Inst.* **33**, 1113–1120.

Lefebvre, A. H. 2010 *Gas Turbine Combustion*. CRC Press.

Lieuwen, T. C. 2012 *Unsteady Combustor Physics*. Cambridge University Press.

Mejia, D., Selle, L., Bazile, R. & Poinsot, T. 2014 Wall-temperature effects on flame response to acoustic oscillations. *Proc. Combust. Inst.* .

Moureau, V., Lartigue, G., Sommerer, Y., Angelberger, C., Colin, O. & Poinsot, T. 2005 Numerical methods for unsteady compressible multi-component reacting flows on fixed and moving grids. *J. Comput. Phys.* **202**, 710–736.

Nicoud, F., Baya Toda, H., Cabrit, O., Bose, S. & Lee, J. 2011 Using singular values to build a subgrid-scale model for large eddy simulations. *Phys. Fluids* **23**, 85–106.

Piacentini, A., Morel, T., Thevenin, A. & Duchaine, F. 2011 Open-palm: an open source dynamic parallel coupler. In *IV International Conference on Computational Methods for Coupled Problems in Science and Engineering*.

Poinsot, T. & Lele, S. 1992 Boundary conditions for direct simulations of compressible viscous flows. *J. Comput. Phys.* **101**, 104–129.

Poinsot, T., Veynante, D., Bourienne, F., Candel, S., Esposito, E. & Surjet, J. 1988 Initiation and suppression of combustion instabilities by active control. In *22nd Symp. (Int.) on Combustion*, pp. 1363–1370. The Combustion Institute, Pittsburgh.

Sattelmayer, T. & Polifke, W. 2003 Assessment of methods for the computation of the linear stability of combustors. *Combust. Sci. Tech.* **175**, 453–476.

Schmid, P. J. 2010 Dynamic mode decomposition of numerical and experimental data. *J. Fluid Mech.* **656**, 5–28.

Schmitt, P., Poinsot, T., Schuermans, B. & Geigle, K. P. 2007 Large-eddy simulation and experimental study of heat transfer, nitric oxide emissions and combustion instability in a swirled turbulent high-pressure burner. *J. Fluid Mech.* **570**, 17–46.

Schönfeld, T. & Rudgyard, M. 1999 Steady and unsteady flow simulations using the hybrid flow solver AVBP. *AIAA J.* **37**, 1378–1385.

Searby, G. 1992 Acoustic instability in premixed flames. *Combust. Sci. Tech.* **81**, 221–231.

Searby, G., Habiballah, M., Nicole, A. & Laroche, E. 2008 Prediction of the efficiency of acoustic damping cavities. *J. Propul. Power* **24**, 516–523.

Sjunnesson, A., Henrikson, P. & Löfström, C. 1992 Cars measurements and visualization of reacting flows in a bluff body stabilized flame. *28th Joint Propulsion Conference and Exhibit AlAA 92-3650* **92**.

Sjunnesson, A., Nelsson, C. & Max, E. 1991*a* Lda measurements of velocities and turbulence in a bluff body stabilized flame. *Proceedings of 4th International Conference on Laser Anemometry* **3**, 83–90.

Sjunnesson, A., Olovsson, S. & Sjoblom, B. 1991*b* Validation rig – A tool for flame studies. In *International Symposium on Air Breathing Engines, 10 th, Nottingham, England*, pp. 385–393.

Tay-Wo-Chong, L. & Polifke, W. 2013 Large eddy simulation-based study of the influence of thermal boundary condition and combustor confinement on premix flame transfer functions. *J. Eng. Gas Turb. and Power* **135**, 021502.